P53 mutations in sporadic and NF1 related malignant peripheral nerve sheath tumors (MPNST): from clinical evidences to a molecular rationale

M. Ferrone[1], S. Pricl[1], M.S. Paneni[1], E. Tamborini[2], S. Pilotti[2], M.A. Pierotti[3]

[1]*Computer-aided System Laboratory, Department of Chemical, Environmental and Raw Materials Engineering, University of Trieste – Piazzale Europa 1, 34127 Trieste, Italy*
URL: www.caslab.units.it e-mail: ferrone@dicamp.units.it

[2]*Experimental Molecular Pathology, Department of Pathology, Istituto Nazionale per lo Studio e la Cura dei Tumori, Via Venezian 1, 20133 Milano, Italy*

[3]*Department of Experimental Oncology, Istituto Nazionale per lo Studio e la Cura dei Tumori, Via Venezian 1, 20133 Milano, Italy*

TP53 encodes p53, a nuclear phosphoprotein with cancer-inhibiting properties. Mutations in the p53 are associated with more than 50% human cancers, and 90% of these affect p53-DNA interactions, resulting in a partial or complete loss of transactivation functions. In a recent cohort study conducted at the Istituto Nazionale per lo Studio e la Cura dei Tumori of Milan, p53 mutations were detected in 9% of NF1 MPNSTs and 43% of sporadic MPNSTs. In particular, for the first time the missense mutation located at exon 7, resulting in the corresponding C238Y point mutation on the p53 protein, was discovered. In order to generate a molecular model, able to support the experimental evidence and to yield a rationale for the molecular implications in MPNSTs, we performed free energy perturbation-based molecular dynamic simulations on different p53 mutant structures. The model has been validated against experimental data, and subsequently used for structure/property relationship prediction in the case of the p53 C238Y mutation.

Keywords: P53, MPNST, mutations, free energy calculations, molecular modeling

1 INTRODUCTION

It is becoming accepted that the progression of mammalian cells towards malignancy is an evolutionary process that involves an accumulation of mutations on both the molecular and chromosomal level. Inherent in models for malignant progression is the concept that an initial mutation in an important regulatory gene (protein) may be pivotal in this process. Once the initial mutation is introduced, loss of normal gene function or the acquisition of deleterious functions may lead to additional mutations furthering the malignant transformation of the cell [1]. Wild-type protein p53 (Figure 1) encoded by the so-called tumor suppressor gene maintains the integrity of the genome during cell division. For this reason it is a good candidate for the involvement in this process. It is estimated that, out of the 6.5 million people diagnosed each year with some form of cancer, about one half have p53 mutations in their tumor cells, and that the vast majority of these are single point mutations [2,3].

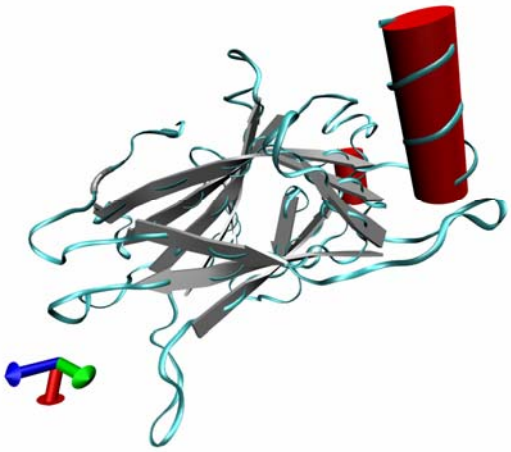

Fig. 1 Crystal structure of p53 (PDB code: 1TSR).

90% of mutations in the p53 affect p53-DNA interactions, resulting in a partial or complete loss of transactivation functions. Malignant peripheral nerve sheath tumors (MPNSTs) encompass a wide group

of neoplasms with Schwann cell differentiation features. They arise either sporadically or in association with neurofibromatosis type 1 (NF1). In a recent cohort study conducted at the Istituto Nazionale per lo Studio e la Cura dei Tumori of Milan (INSCT), p53 mutations were detected in 9% of NF1 MPNSTs and 43% of sporadic MPNSTs. As mentioned above, for the first time C238Y point mutation on the p53 protein, was discovered. In particular, this discovered was obtained during the analysis of 28 cases of both MPNSTs and/or neurofibromas, subdivided into 14 NF1-unrelated cases. INSCT studied the structural and functional alterations of the p53, and the immunophenotypic expression of their relative products [4].

In theory, it should be possible to restore at least some functional activity of p53 mutants by enhancing the stability of the protein in its folded state, and/or providing additional DNA contacts. However, so far, the exploitation of the available clinical data has been hampered by our limited understanding of the structural and functional characteristics of the individual p53 mutants.

In this work we present here one attempt to exploit the knowledge available on p53 protein structure and the power of sophisticated molecular modeling techniques to classify the various types of mutants into specific categories and to understand the structural effect of the new INSCT discovered point mutations C238Y. Accordingly, the following 10 cancer-associated mutants that are distributed throughout the core domain and are representative of the p53 mutation database have been considered and modeled: R248Q R273H F134L G245S R249S R282W R175H M237I C242S and C238Y.

2 MODELING DETAILS

2.1 The thermodynamic cycle

To explain the free energy (FE) simulation method, in Figure 2 we report the thermodynamic cycle, where WT_N, WT_D, M_N and M_D, represent the wild-type protein in the native state, in denatured state, the mutant in the native state and in denatured state, respectively.

A measure of the denaturation free energy changes of the wild-type, $\Delta G_{U,WT}$, and of the mutant proteins, $\Delta G_{U,M}$ can be obtained experimentally by calorimetry techniques [5]. The free energy simulations, in which one residue is changed into another during the calculation for the folded/unfolded state, yields the values of $\Delta G_{N,WT/M}$ and $\Delta G_{D,WT/M}$.

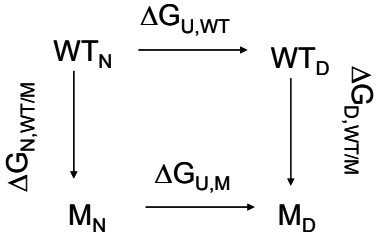

Fig. 2. Thermodynamic cycle.

According to the thermodynamic cycle, the simulation results can be related to the experimental evidences by: [6].

$$\Delta\Delta G = \Delta G_{U,WT} - \Delta G_{U,M} = \Delta G_{N,WT/M} - \Delta G_{D,WT/M} \quad (1)$$

2.2 Computational procedure

The simulations were carried out with the AMBER 6.0 suite of programs.[7] The initial 3-D structure of the wild-type p53 was taken as chain B of PBD entry 1TSR. Hydrogens were added to the protein backbone and side chains using the PROTONATE module at pH = 7. The non-bonded model for the zinc ion was adopted [8]. The hydrogen atoms were then minimized for 200 steps (steepest descent) in vacuum using the SANDER module and the Cornell et al. force field.[9] The p53 was immersed in a 55-Å radius sphere of TIP3P-water molecules, and the system was minimized with a gradual decrease in the position restraints of the protein atoms. The appropriate number of counterions (Na^+ and Cl^-) was placed next to solvent exposed charge residues. A 18-Å radius spherical cap of TIP3P-water molecules was then centered around the initial position of Cβ of each wild type residue that undergoes a point mutation. The water cap was equilibrated for 50 ps at 283 K, keeping the protein and hydrating water molecules outside the water cap rigid. Next, the system was heated for 50 ps and equilibrated for 300 ps at 283 K. Since X-ray/NMR structures of mutant p53 molecules have not been reported yet, the initial structures for the mutant p53 simulations were prepared using InsightII (from Accelrys, San Diego CA, USA) by swapping the mutant residue into the specific site [10]. Starting mutant side chain orientation was selected using the side chain rotamer library method. All Molecular Dynamics simulations and energy minimizations were performed again with the SANDER module. All simulations were

carried out with a time step of 1 fs. During these simulations, only those residues and water molecules within 18 Å of the center of mass of the Cβ of the point mutation atom were allowed to move with the use of the BELLY module. The SHAKE algorithm was applied on all bonds containing hydrogens. For each simulation the temperature was controlled at 283 K by coupling of the system to a heat bath [11], periodical boundary conditions were applied and the pressure was controlled at 1 atm using weak coupling. The denatured state simulations we assumed a tripeptide model of sequence AXB, in which A and B were the amino acid residues preceding and following the mutating residue X, respectively. Each tripeptide was blocked by a CH_3 group prior to residue A and a $NHCH_3$ group following residue B. The globally resulting tetrapeptide was placed in a box of 736 water molecules, and the system was equilibrated for 50 ps with all the same conditions of the previous. Finally, the free energy calculations were carried on these systems. In all simulations, a total time of 40 ps was used in each direction of the thermodynamic cycle with a time step of 1 fs. The perturbation group was assumed to be the whole mutant residue, but only interactions occurring between this residue and other residues were included in the free energy evaluation.

3 RESULTS AND DISCUSSION

3.1 Experimental evidences

To warrant a detailed discussion of protein stability it is fundamental to perform a comparison of the protein structures in the simulations with the related experimental structure. The first check we performed was the analysis of the root-mean-square deviations (RMSD) from the initial structure of the protein backbone atoms that are moving during the simulation. We obtained RMSD values fluctuating between 1.2 and 1.4 Å, in harmony with those found in other protein simulations [12]. This confirmed that, overall, the simulation protocol adopted did not cause significant drift of WT p53 from its initial structure. In the same way, we then compared the RMSDs of the backbone atoms of the resulting p53 mutants with the equilibrated WT p53 model structure.

Table 1 reports the results obtained from the free energy calculations against the experimental data. An inspection of this Table reveals that the calculated results are of the observed sign (wild type more stable than mutants) and have a magnitude close to the experimental values in all cases. Moreover the statistical error in the simulations is of the order of a few tenths of kcal/mol so MD/FE appear sufficiently accurate to be used for obtaining information about the difference in stability of the protein conformations under consideration, and to permit analysis of the origin of these differences.

Table 1. Calorimetric experimental free energy of denaturation and total free energy change calculated by MD/FE for different p53 mutant.

Mutations	ΔΔGexp (kcal/mol)	ΔΔGcal (kcal/mol)
R248Q	1.87±0.09	2.04±0.14
R273H	0.45±0.04	0.22±0.15
F134L	4.78±0.08	4.90±0.11
G245S	1.21±0.03	1.50±0.19
R249S	1.92±0.04	2.20±0.15
R282W	3.30±0.10	3.42±0.16
R175H	3.52±0.06	3.69±0.11
M237I	3.18±0.06	3.30±0.14
C242S	3.07±0.05	3.27±0.15
C238Y	-	3.20±0.17

Following energetic data validation, we analyzed he structural effect of each single point mutation on p53. Here, for the sake of brevity, we will discuss only two mutations: R248Q and C238Y.

R248Q is a hotspot mutation positioned in loop3 of p53. R248 makes a fundamental DNA minor groove contact, and is one of the most solvent exposed groups. In the structure of the native P53, R248 is involved in a persistent, fundamental H-bond with S240 (average dynamic length ADL = 2.6Å), which lies between the two Zn^{++} ligands, C238 and C242. This no longer exists in Q248. We have quantified the loss energy related with H-bond by turning off the partial charges of the R248 NH group. The resulting energy difference is about 0.8 kcal/mol. This is in agreement with the non bond terms calculated for ΔΔGcalc, 1 kcal/mol and 0.8 kcal/mol for electrostatic and van der Waals contributions, respectively. Further, the latter value is in harmony with the side truncation of an exposed CH_2 (difference in solvent accessible surface = 16 $Å^2$).

C238Y is a single point mutation discovered for the first time at INSCT. It belongs to loop3, and is directly involved in Zn^{+2} binding. In Table 2 we report the energy terms calculated with the MD/FEP approach.

This mutation drastically changes the region, resulting in the strong distortion of the Zn^{+2} coordination site. This is principally due to the

dimensions of the new residue T, characterized by a molecular surface of approximately 205 Å^2, constrained in a narrow place. Besides, these evidences are supported by the drastic change in hydrophobicity, from 2.5 of C to -1.3 of T, respectively.

Table 2. free energy change for the C238Y mutation calculated by MD/FE.

kcal/mol	electrostatic	van der Waals
ΔGn	5.21	4.56
ΔGd	3.99	2.58
ΔΔG	1.22	1.98

4 CONCLUSIONS

The good agreement between calculated and experimental ΔΔG values has proven that MD/FE methods can be used to analyze the effect of protein stability of site-specific mutation. Further, using dedicated simulation procedures we can unambiguously compute both the electrostatic and the vdW contribution to ΔΔG and, by resorting to further techniques, such as the zeroing of the molecular partial charges, we get new insight into protein stability.

ACKNOWLEDGMENTS

We acknowledge the generous financial support from AIRC, grant 2955 "Pathogenetic pathways determining pharma-cological response: a novel tumoral functional classification approach" (2004). We are also grateful to UCSF for providing Amber 6.0.

REFERENCES

1. S. Pricl, M. Fermeglia, M. Ferrone, E. Tamborini, M. Oggioni, F. Perrone, S. Pilotti, D. Delia and M.A. Pierotti, Detailed Computational Study of point mutations of the TP53 tumor-suppressor protein, In *Proceedings of the 2002 ACS,* Boston, USA, (2002), CD ROM paper 38.
2. N.P. Pavletich, K.A. Chambers and C.O. Pabo, The DNA-binding domain of p53 contains the four conserved regions and the major mutation hot spots, *Genes Develop.* 7 (1993), 2556.
3. C. Branden and J. Tooze, *Introduction to protein structure*, 2nd ed. Garland Publishing, New York (1999).
4. S. Birindelli, F. Perrone, M. Oggioni, C. Lavariono, B. Pasini, B. Vergani, G.N. Ranzani, M.A. Pierotti and S. Pilotti, Rb and TP53 pathway alterations in sporadic and NF1-related malignant peripheral nerve sheath tumors, *Lab. Invest.* 81 (2001) 833-834.
5. A.N. Bullock, J. Henckel, A.R. Fersht, Quantitative analysis of residual folding and DNA binding in mutant p53 core domain: definition of mutant states for rescue in cancer therapy, *Oncogene* 19 (2000) 1249.
6. S. Pricl, M. Fermeglia, M. Ferrone, E. Tamborini and S. Pilotti, Science (2004), submitted.
7. D.A. Case, D.A. Pearlman, J:W. Caldwell, T.E. Cheatham III, W.S. Ross, C.L. Simmerling, T.A. Darden, K.M. Merz, R.V. Stanton, A.L. Cheng, J.J. Vincent, M. Crowley, V. Tsui, R.J. Radmer, Y. Duan, J. Pitera, I. Massova, G.L. Seibel, U.C. Singh, P.K. Weiner, P.A. Kollman, AMBER 6, (1999), University of California, San Francisco, CA, USA.
8. O.A.T. Donini and P.A. Kollman, Calculation and prediction of binding free energy for the matrix metalloproteinases, *J. Med. Chem.* 43 (2000) 4183.
9. W. Cornell, P. Cieplak, C.I. Bayley, I. Gould, K.M. Merz, D.M. Ferguson, D.C. Spellmeyer, T. Fox, J.W. Caldwell and P.A. Kollman, A second generation force field for the simulation of proteins and nucleic acids, *J. Am. Chem. Soc*. 117 (1995) 5179.
10. S.C. Lovell, The penultimate rotamer library, *Proteins: Struct. Funct. Genet*. 40 (2000) 389
11. H.J.C. Berendsen, J.P.M. Postma, W.F. van Gunsteren, A. DiNola, J.R. Haak, Molecular dynamics with coupling to an external bath, *J. Chem. Phys*. 81 (1984) 3684.
12. I. Chandrasekhar, G.M. Clore, A. Szabo, A.M. Gronenborn, B.R. Brooks, 500 ps molecular dynamics simulation study of interleukin-1beta in water, *J. Mol. Biol*. 226 (1992) 241.